Hydrogeol J (2016) 24:1463–1478
DOI 10.1007/s10040-016-1419-6

PAPER

Improved regional groundwater flow modeling using drainage features: a case study of the central northern karst aquifer system of Puerto Rico (USA)

Reza Ghasemizadeh[1] · **Xue Yu**[1] · **Christoph Butscher**[2] · **Ingrid Y. Padilla**[3] · **Akram Alshawabkeh**[1]

Received: 19 August 2015 / Accepted: 14 April 2016 / Published online: 30 April 2016

Abstract In northern Puerto Rico (USA), subsurface conduit networks with unknown characteristics, and surface features such as springs, rivers, lagoons and wetlands, drain the coastal karst aquifers. In this study, drain lines connecting sinkholes and springs are used to improve the developed regional model by simulating the drainage effects of conduit networks. Implemented in an equivalent porous media (EPM) approach, the model with drains is able to roughly reproduce the spring discharge hydrographs in response to rainfall. Hydraulic conductivities are found to be scale dependent and significantly increase with higher test radius, indicating scale dependency of the EPM approach. Similar to other karst regions in the world, hydraulic gradients are steeper where the transmissivity is lower approaching the coastline. This study enhances current understanding of the complex flow patterns in karst aquifers and suggests that using a drainage feature improves modeling results where available data on conduit characteristics are minimal.

Keywords Groundwater flow · Conduit drainage · Karst · Discharge hydrograph · Puerto Rico (USA)

✉ Akram Alshawabkeh
aalsha@coe.neu.edu

[1] Department of Civil and Environmental Engineering, Northeastern University, Boston, MA 02115, USA

[2] Department of Engineering Geology, Institute of Applied Geosciences, Karlsruhe Institute of Technology, 76131 Karlsruhe, Germany

[3] Department of Civil Engineering and Surveying, University of Puerto Rico, Mayaguez, PR 00682, USA

Introduction

Aquifers in karst regions represent some of the most challenging aquifers to characterize due to their heterogeneity caused by enlarged conduit networks in fractured rock. Groundwater flow is governed by well-understood hydraulic behavior through porous media, but has been more difficult to delineate when passing through fissured media with conduits of prevailing non-Darcian flow. The hydrodynamic behavior, contaminant fate and transport, and monitoring and remediation activities in karst aquifers all involve high uncertainty levels often due to limited field data and lack of characterization techniques applicable to heterogeneous media (Smart and Hobbs 1986; Rodriguez-Martinez 1997).

Karstification commonly enhances aquifer permeability through dissolution of carbonate rocks resulting in self-organized subsurface channel networks formed by positive feedback between dissolution and flow (Worthington and Ford 2009). Besides the spacing of rock fractures and the magnitude of the hydraulic gradient, the aperture variability and recharge conditions are the most important factors influencing channel networks enlargement (Lauritzen et al. 1992; Kaufmann and Braun 1999). Karst conduits exhibit many different patterns depending on local geology and the flow field characteristics (White 2003). Conduits commonly provide a link between sinkholes, or sinking streams, and productive springs.

Previous research has attempted to address the complex spring flow behavior in karst systems. White (1969) established a comprehensive conceptualized physical framework for characterizing karst groundwater systems. Based on dissolved carbonate species in spring water, Shuster and White (1971) categorized karst aquifers into conduit flow and diffuse flow feeder-systems demonstrating high variability and low variability in temperature and carbonate hardness

throughout the year, respectively. While this classification was true for their study area, further investigations in other geological settings suggest that almost all carbonate springs are mostly conduit springs (e.g. Worthington 1991; Schindel et al. 1996). White (2002) later stated that low-variability springs are fed by dispersed recharge, with variations in chemistry and temperature being buffered largely in the soil zone, so there is no reason why these springs should not have associated extensive conduits. Worthington (1991) distinguished between springs that carry the base flow from groundwater basins (underflow springs) and those that carry only part of the discharge or become active only during storm events (overflow springs).

Conduit sizes range from centimeters to tens of meters, with conduits acting as low-hydraulic-resistance storm drains, extracting water from the surrounding matrix and fracture system (White 2003). A large majority of karst aquifers have such conduit networks where flow is typically in the turbulent regime, and groundwater velocities can exceed 100 m/d.

Ghasemizadeh et al. (2012) provided a comprehensive description of different modeling approaches specifically developed for flow and transport in karst environments, and identified criteria to choose the appropriate approach based on available data and the purpose of the study. Lumped parameter models treat karst aquifers as sets of reservoirs and constrictions to reproduce the response of conduit systems at the field scale while ignoring the complexity of the aquifer structure (Wanakule and Anaya 1993; Lee and Krothe (2001); Kovacs (2003); Jukić and Denić-Jukić 2009; Butscher et al. 2011). Distributed modeling approaches simplify the karst structure (Liedl et al. 2003; Scanlon et al. 2003; Sauter et al. 2006; Graf and Therrien 2007; Weatherhill et al. 2008)—for example the equivalent porous media (EPM) approach treat conduits as high permeability regions. Some researchers have used special boundaries such as constant head boundary which can exchange water into and out of the aquifer at a rate proportional to the hydraulic head difference (e.g. Angelini and Dragoni 1997; Dufresne and Drake 1999) or head-dependent drain to reproduce the spring discharge in karst systems based on head differences between the spring pool and the surrounding potentiometric surface (e.g. Yobbi 1989; Scanlon et al. 2003; Quinn et al. 2006). This approach uses a high drain conductance to allow for unrestricted water discharge from the aquifer matrix into the conduit system.

Quinn et al. (1998) simulated conduits in mixed-flow systems by assigning connected pathways of drain cells between inlet sinkholes or tracer release locations and outlet springs. More recently, Papadopoulou et al. (2010) used the drain feature to approximate the hydraulic behavior of a faulted complex karst aquifer system, where two major geological discontinuities (faults) dominate the regional subsurface flow and remarkably deplete the aquifer in adjacent areas. The length and orientation of dominant faults were found to affect the flow field, especially during the rainy season. Where more detailed geologic data were available, Peterson and Wicks (2006) evaluated the importance of conduit geometry and hydraulic parameters on controlling transport dynamics within karst. They estimated the strength of storm water management model (SWMM) for simulating local solute transport to be satisfactory but limited. Implementing drains to represent the conduit network is challenging since information about the spatial distribution and geometry of the network are rarely known. Conceptual considerations suggest that conduit features are correlated to superficial features: recharge from surface runoff is concentrated in topographical depressions, enhancing carbonate dissolution in the geological subsurface leading to the development of karst conduits. Solutionary-formed fracture systems act as conduits and have contributed to conduit controlled paths, closed sinkhole depressions, and dry valleys (Renken et al. 2002).

Eisenlohr et al. (1997) numerically simulated the theoretically defined karst structures using a double porosity approach—with a high hydraulic conductivity channel network embedded in low hydraulic conductivity fractured rock—to analyze spring responses. This work led to a conceptualization of the spring hydrograph as a function of several factors, such as occurrence and extent of flooding events, the frequency of hydrological events during the period analyzed, and the type of recharge processes (i.e., the ratio of diffuse to concentrated infiltration). Worthington (2009) used highly conductive cells to simulate karst conduits in the Mammoth Cave aquifer, resulting in more accurate predictions than without considering conduits; however, hydraulic conductivity and therefore flow velocities were underestimated because conduits of up to a few meters wide were approximated with cells of 200-m width and 100-m height.

Indeed, the karst hydrology models are significantly hindered by the complexity of conduit drainage systems especially conduit flow path and limitations in field data. There is a scientific gap in the literature in simulating the drainage effects of conduit networks where only little information on physical characteristics and geologic setting is available. It is hypothesized that by assigning simulated drainage lines connecting conduits to springs, EPM modeling abilities can be significantly improved. To test this hypothesis, the steady-state hydrogeology of the upper karst aquifer system in central northern Puerto Rico (NPR) and the natural drainage features including major springs and surface water bodies within the karst aquifer system were explored. The strengths and limitations of the improved EPM approach in simulating the transient spring discharge are evaluated. As the next objective of the work, the variation of groundwater head in springs' catchment area and some of the spring responses to rainfall events are assessed to better describe their behavior. It is also an

objective of this paper to evaluate the dependency of hydraulic conductivity field data on the measurement scale in Puerto Rico and to compare it to other karst systems in the world.

Materials and methods

Study area

General geology

The study area is located between the two rivers Rio Camuy and Rio de la Plata in NPR and includes, from west to east, the municipalities of Camuy, Hatillo, Arecibo, Barceloneta, Manati, Vega Baja, Vega Alta, and Dorado (Fig. 1). The colors on the map depicted in Fig. 1 indicate the land surface elevation using a digital elevation model (DEM) from the National Elevation Dataset (NED) from the US Geological Survey (USGS).

In central NPR, land surface altitudes range from sea level in the north to about 300 m above sea level (a.s.l.) to the south in the karst uplands (Fig. 1). The hydrogeologic framework includes an unconfined upper aquifer (i.e., Aymamon and Aguada Limestone), a confined lower aquifer (i.e., San Sebastian Formation and Lares Limestone), and an intermediate confining unit (i.e., Cibao Formation and Montebello Limestone) separating the two hydraulically independent aquifers (Fig. 2). Fractures tend to be closed in the deeper subsurface due to higher pressure and are expected to be open and more numerous where the Cibao Formation lies near the surface. The upper aquifer is contained within the Aguada and Aymamon limestone (from Miocene age) overlaid by alluvial and blanket sand deposits in floodplains and along the coast (Monroe 1976). The average northerly dip of the Aymamon and Aguada interface (Fig. 2) is about 6.5° in the south and about 2° near the coast (Monroe 1980).

Hydrogeology

The coastal limestone aquifer system in NPR is mainly recharged by precipitation that enters through limestone cropouts in the southern karst uplands. In the upper aquifer, groundwater discharges to the major rivers, wells, coastal wetlands, lagoons, near shore and offshore springs, or as seabed seepage directly to the sea (Cherry 2001; Torres-González 1985; Torres-González et al. 1996; Gomez-Gomez and Torres-Sierra 1988; Sepúlveda 1999). There are 119 private and public pumping wells in the study area controlled by Puerto Rico Aqueduct and Sewer Authority (PRASA). Most of Puerto Rico's rainfall is orographic; moist ocean air moves inland where it cools down adiabatically over the mountains and condenses in the form of rain (Calvesbert 1970). The shoreline in the north of Tortuguero lagoon is irregular from west to east causing uneven seaward discharge patterns. Freshwater moves seaward above the transition zone with sea water, and its discharge interface with the sea is up to a few hundred meters wide (Bennett and Giusti 1972).

Although the upper aquifer of the north coast appears to be best characterized as a diffuse-flow carbonate aquifer, it seems likely that groundwater flow in the upper aquifer is partially controlled by regional fractures (Renken et al. 2002). Abundance of major springs and outcropping water-bearing limestone rocks in NPR suggest that groundwater flow largely occurs through a system of preferential flow paths such as closely spaced conduits and faults (Bennett and Giusti 1972; Giusti 1978). Conduit flow is mostly assigned to a vaguely defined system of dissolution-enlarged fractures within the Aymamón and Aguada limestone of the upper aquifer. Due to existence of high permeability pathways, the NPR karst system is considered highly vulnerable to contamination from Superfund sites within the study area (Yu et al. 2015a, b). The contaminant transport in karst may depend primarily on the karst conduit network rather than matrix hydraulic conductivity.

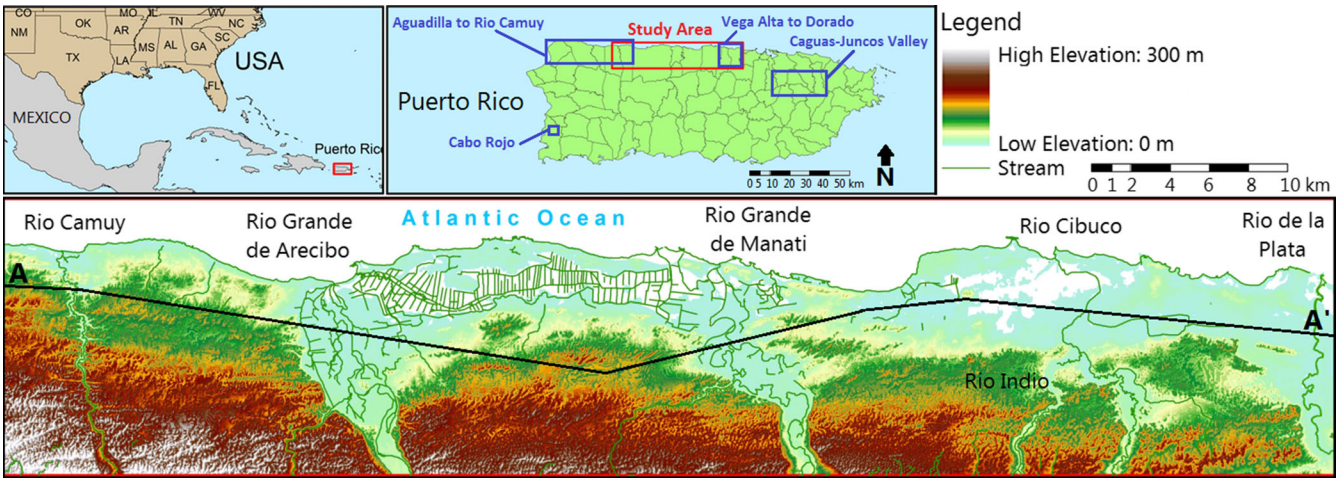

Fig. 1 Location of study area, wetland, major streams, and land surface elevation data of central NPR

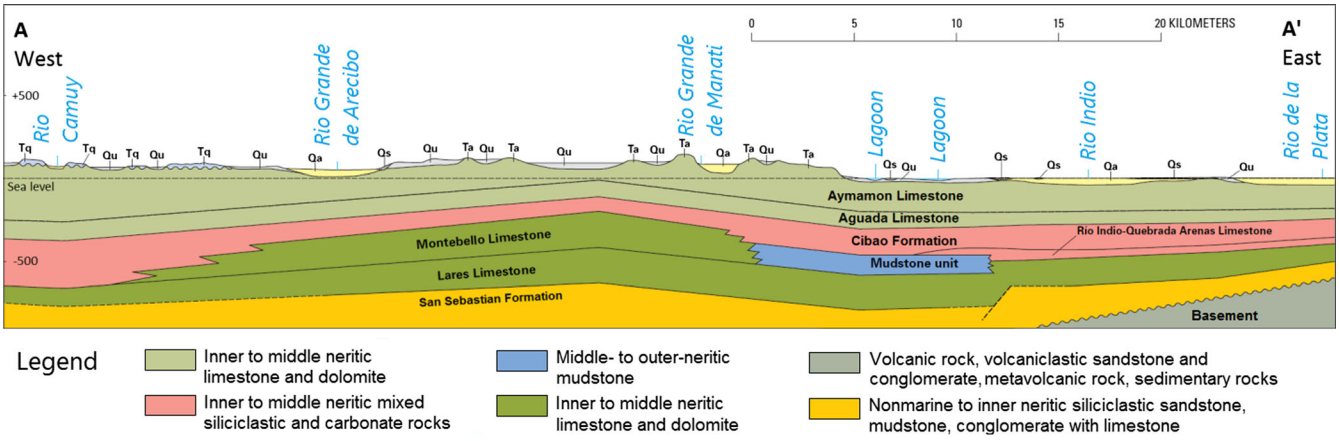

Fig. 2 Geologic formations in the central NPR aquifer system along cross section *A–A′* (modified from Renken et al. 2002). Location of cross-section: see Fig. 1

Surface lineaments

Surface lineaments generally reflect topography, vegetation, and soil tonal alignments (Lattman and Parizek 1964) and distinctly differ from the pattern of adjacent features (O'Leary et al. 1976). Caves and underground drainages have a tendency to extend predominantly along and parallel to the dip direction of the geological units (S–N), and the regional groundwater flow patterns closely follow those trends (White and White 2001; Deike 1969; Hurd et al. 2010). Based on the principles used by Lattman and Parizek (1964) and O'Leary et al. (1976), Briere and Scanlon (2000) interpreted the frequency and occurrence of major lineaments in Puerto Rico and mapped 636 lineaments with different lengths (0.2–25 km, mean length of 2.8 km, and total length of 1,808 km). In their study, the estimated lineaments in NPR are more frequent in some parts and infrequent elsewhere; however, the SLAR images do not suggest major lineaments in the central NPR. Ward et al. (1991) traced more refined lineaments from a 1:140,000 geologic map (Monroe 1980) between the Río Grande de Arecibo and Río Grande de Manatí, where major fracture patterns are along the strike of surface lineaments in karst topography with varying, mostly SSW–NNE-trending orientation. Sinkholes (Alemán-Gonzalez 2010) and springs (Rodriguez-Martinez 1997) in NPR occur along and at the end of lineaments.

Conduit flow

Hydrological investigations suggest that water-bearing conduits are present in northwestern Puerto Rico between the Aguadilla and Rio Camuy area (Giusti and Bennett 1976; Rodríguez-Martínez 1995). Conduit flow is negligible within the western half of the modeling domain used here (Torres-González et al. 1996). Rodriguez-Martinez (1997) categorized some of the springs in NPR into diffuse-type and conduit-type springs with primarily seasonal fluctuation and strong short-term variation in discharge and water quality in direct response to rainfall, respectively (Table 1). The high variability in field-measured transmissivity suggests existence of fracture zones and dissolution channels between Rio Grande de Manati and Rio Indio area (Cherry 2001), which is in agreement with three major springs in that area classified as conduit-type by Rodriguez-Martinez (1997). Although there

Table 1 Characteristics, coordinates, and elevation of major springs in the central NPR. *C* conduit type; *D* diffuse type

No.	Spring Name	Elevation (m a.s.l.)	Type[a]	Order	Municipality	Latitude (N)	Longitude (W)
1	Ojo de Guillo	1.68	C	3	Manati	18°25′41″	66°31′36″
2	Isidro (Tierras Nuevas)	0.91	C	4	Manati	18°28′04″	66°30′16″
3	Laguna South	0.46	C	3	Manati	18°27′37″	66°27′07″
4	Maguayo	15.03	C	4	Dorado	18°24′46″	66°15′55″
5	Palo de Pana and Mamey	1.83	D	4	Manati	18°27′59″	66°30′41″
6	Ojo de Agua	1.31	D	3	Vega Baja	18°26′57″	66°25′06″
7	Mackovic	–	D	4	Vega Alta	18°27′58″	66°22′26″

[a] As proposed by Rodriguez-Martinez (1997)

are no major conduits or springs between Rio Indio and Rio de la Plata (Sepúlveda 1999), Maguayo spring in Dorado was classified as conduit-type based on field flow measurements (Rodriguez-Martinez 1997). Diffuse-type springs show less carbonate hardness and temperature variation throughout the year and receive less contribution from conduits and more from small fractures and matrix flow discharge. Conduit-type springs rapidly drain aquifers and provide little attenuation to storm-water recharge, thus posing higher intrinsic vulnerability of karst groundwater to short-lived contaminants (Butscher et al. 2011).

Highly productive springs within the coastal limestone aquifer system in NPR are described by Guzmán-Ríos (1988). According to the classification system developed by Meinzer (1927), springs are categorized based on their discharge into orders (first to eighth), with greater than 245,000, 24,640–246,400, 2,460–24,640, 550–2,460, 55–550, 5.5–55, 0.7–5.5 m^3/d, and less than 0.7 m^3/d, respectively. Out of the 67 identified springs in the NPR coastal limestone belt, 10 are third order, 4 are fourth order, 14 are fifth order, 19 are sixth order, 6 are seventh order, and 14 are eighth order, which normally are dry and only active after rainfall (Rodriguez-Martinez 1997). Most springs that discharge from the upper aquifer are third order or fourth order springs (Lugo et al. 2001) and there is no first, second, or fifth order spring within the hydrologic system of this study area (Table 1). There are seven third or fourth order springs considered in this study as listed in Table 1. Sixth or higher order springs are not considered in this study because of their low discharge and insignificant effect on regional groundwater flow. Karst springs within the lower aquifer (such as Aguas Frias, the largest spring in Puerto Rico, fed by Rio Encantado Cave) are not included in the model.

Among the springs classified as conduit-type and diffuse-type by Rodriguez-Martinez (1997) in the study area (Table 1), continually measured field data were only available for two gaged springs, Oje de Agua and Oje de Guillo, with discharges measured by the USGS between 1993 and 1996.

Modeling scheme

The groundwater model of the NPR aquifer system was developed using the advanced graphical pre- and post-processing program Groundwater Modeling System (GMS v.10, Aquaveo 2014), which is based on the code MODLFOW (Mcdonald and Harbaugh 1988). While generally large-scale simplifications are necessary in an EPM approach, the present model retains more complexity by considering conduit drainage represented by drain cells. The data are collected from the literature, historical studies, and USGS and entered to the model domain with defined boundaries. After the model parameters recharge and hydraulic conductivity

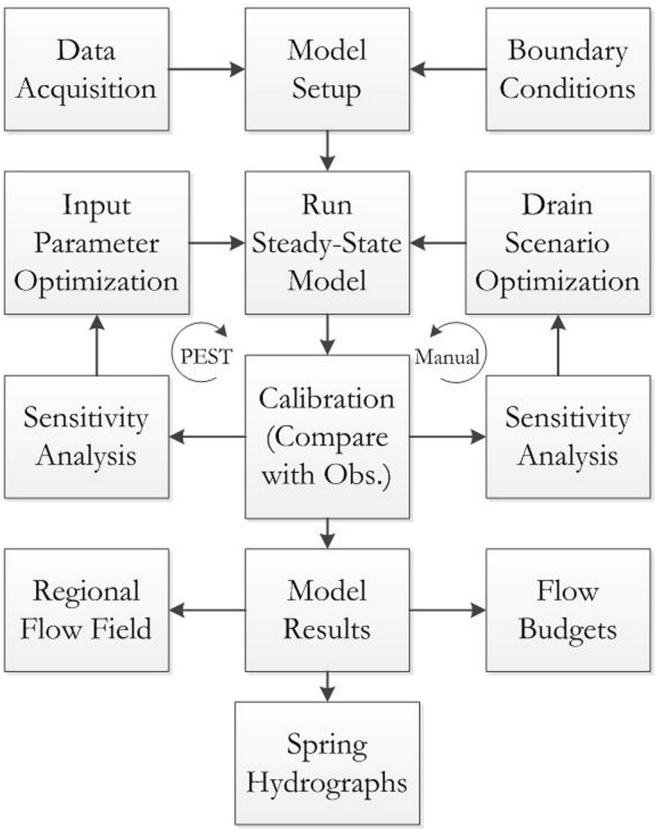

Fig. 3 Groundwater modeling scheme used in this study

have been satisfactorily calibrated using the parameter estimation routine PEST (Doherty et al. 1994), alternative scenarios for direction and location of conduit networks are defined and then evaluated using the drainage feature along with manual calibration (Fig. 3).

Scale effects

Regional (large scale) hydraulic tests (e.g., long-term pumping tests) evaluate the transmissivity over larger distances and therefore increase the likelihood of intersecting highly permeable features (i.e. conduits and fractures) compared to local (small scale) tests (e.g., pulse and slug tests; Rovey 1994); therefore, transmissivities evaluated at large scales tend to be higher than those measured at small scales—e.g. at a regional scale the equivalent hydraulic conductivity tends to be higher in fractured aquifers (Garven 1995). This behavior is called scaling effect (Kiraly 1975; Neuman 1990), which was reproduced on a theoretical basis by Snow (1965), also applies to porosity and storage coefficients (Teutsch and Sauter 1991). Field-geological testing samples a larger heterogeneous rock volume than laboratory tests; therefore, field results are more appropriate for modeling studies at the regional scale than at the local scale.

The scale effect on hydraulic conductivities of the karst aquifer systems in Puerto Rico are illustrated in Fig. 4; where effective test radius indicates the radius of influence (capture area) of pumping wells. Hydraulic conductivity data are determined and effective radii are calculated for four karst aquifers around the island using slug test results (e.g. withdrawal, drawdown, casing screened interval, and radius of casing) from the literature. A total of 29, 20, 13, and 6 individual tests data are extracted from Caguas-Juncos Valley (Puig et al. 1993), Vega Alta to Dorado (Sepúlveda 1999), Aguadilla to Rio Camuy (Tucci and Martínez 1995), and Cabo Rojo (Rodríguez-Martínez 1996) aquifers in eastern, northern, northwestern, and southwestern Puerto Rico, respectively. Similar to other karst systems worldwide, hydraulic conductivity increases with the measuring scale in karst aquifers of Puerto Rico, reflecting the highly heterogeneous nature of the Puerto Rican karst aquifers. Governed by variously scaled field tests, such trends can also be used to validate the selected optimized conductivity values under the EPM approach.

Presented as gray solid lines in Fig. 4, Worthington (2009) provided a summary of previous studies on Yucatan Peninsula (Mexico), Smithville Karst (Ontario, Canada), Jura Mountains (Switzerland), Swabian Alb (Germany), Chalk Karst (England, UK) and Edwards Aquifer (Texas, USA) to illustrates how hydraulic conductivity varies with test radius in other karst aquifers around the world compared with Mammoth Cave (Kentucky, USA). In Puerto Rico, most slug tests were carried out at the catchment scale, and no data is available over radial distances less than 1 m or greater than 1,000 m. The slope of the data is positively correlated with

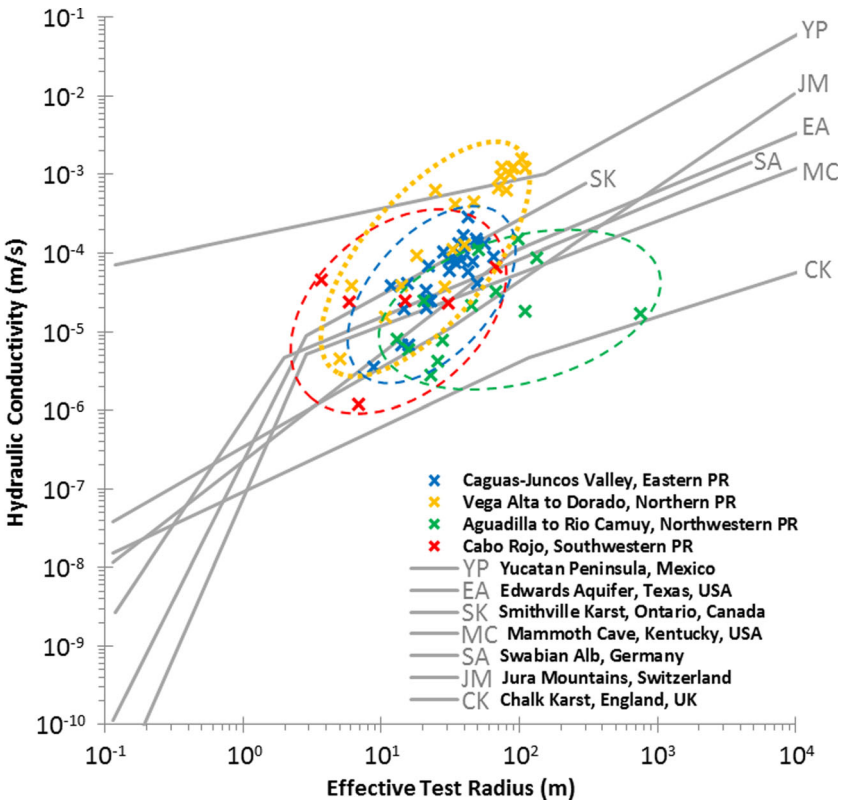

Fig. 4 Hydraulic conductivity of karst aquifers in Puerto Rico (Caguas-Juncos Valley, Puig et al. 1993; Vega Alta to Dorado, Sepúlveda 1999; Aguadilla to Rio Camuy, Tucci and Martínez 1995; Cabo Rojo, Rodríguez-Martínez 1996) as a function of testing scale and comparison with other karsts worldwide (Worthington 2009)

karstification intensity; for example without karstification, the small matrix permeability is equal to bulk permeability. Central NPR is thus the most karstified aquifer in the island, followed by Caguas-Juncos Valley in eastern Puerto Rico.

Model setup

The model domain extends 10.9 km from north to south and 64.6 km from west to east (from 66° 51′ 44″ W to 66° 15′ 03″ W), covering a total of 640 km^2 or 7.3 % of the island's area (Fig. 5). The two-dimensional (2D) model domain is discretized with a uniformly spaced block-centered grid composed of 30 rows and 180 columns (cell size 358.9 m × 363.3 m). A 2D modeling approach was chosen in the present study to simplify the karst aquifers because little or no information on the depth of high permeability pathways is available. The grid is oriented south–north to align with the predominant northward groundwater flow. Flow within the unconfined aquifer is assumed to be horizontal (Dupuit-Forchheimer assumption).

The central NPR karst system is bound by the Atlantic Ocean to the north and outcrops of the Cibao Formation to the south. Underlain by the impermeable Cibao formation toward the south and by the static saltwater interface toward the north (Ghasemizadeh et al. 2015), the aquifer saturated depth spatially varies and is highest where the interface intersects the base of the aquifer. Accordingly, the bottom of the model is the base of the upper aquifer, which is bounded by the freshwater–saltwater interface to the north and the impermeable Cibao formation to the south. A Dirichlet boundary is applied along the northern coastline with constant zero head at the sea level. Predominantly northward groundwater flow, suggested by historical water level data, implies no-flow boundary conditions along the southern, western and eastern boundaries (Fig. 5).

Monthly rainfall data are taken for Manati rain gauge in the study area (MANATI 2 E US, elevation: 250 ft, latitude: 18.431° N, longitude: 66.466° W) from National Oceanic and Atmospheric Administration (NOAA). Considering an evapotranspiration of more than 60 % (Giusti 1978), the average annual recharge rate is about 240 mm in the study area. Aquifer recharge varies spatially based on topography and geologic characteristics, and occurs through infiltration from rivers, limestone outcrops, sinkholes and enclosed topographic depressions. Different recharge rate ranges were initially defined for surficial and geologic units based on those reported by other studies in sub-regions of the study area (Torres-González 1985; Gomez-Gomez and Torres-Sierra 1988; Torres-González et al. 1996; Sepúlveda 1999; Cherry 2001) and then were further adjusted during an automated calibration process.

The highest recharge up to 1.95 mm/d occurs in the southern highland region and in the central permeable outcrop area of the Aguada limestone where limestone is near the surface (Giusti and Bennett 1976). Medium and lower recharge rates correspond to areas with thick blanket deposits and coastal clay deposits, respectively. While the soils in the central part of the study area are well-drained, lowland areas are poorly drained because of blanket sands, and marsh and swamp deposits. Existence of clay layers along the north coast prevents the infiltration to the aquifer, resulting in negligible net recharge (e.g. Torres-González 1985; Torres-González et al. 1996) along the northern coastal plain, and 0.3–1.4 mm/d in the alluvial valleys (e.g. Quinones-Aponte 1986; Torres-González 1985; and Gomez-Gomez and Torres-Sierra 1988). Aerially distributed recharge rates over these zones were then varied monthly during the transient simulations. Although hydraulically independent (Cherry 2001), the unconfined parts of the lower aquifer in the southwestern area provide water to the upper unconfined aquifer. The flux was estimated to be about 19,600 m^3/d by Torres-González et al. (1996), which is considered as a constant influx (implemented as injection wells) along the southwest boundary between Rio Camuy to Rio Grande de Arecibo in the model (Fig. 5). Runoff over the southeastern outcrops in Cibao Formation was estimated to be 3,900 m^3/d by Cherry (2001) and is similarly considered as influx between Rio Grande de Manati to Rio Indio.

No field hydrogeological investigations such as tracer tests, attempted to detect the orientation and distribution of subsurface conduits within the carbonate rocks of the north coast

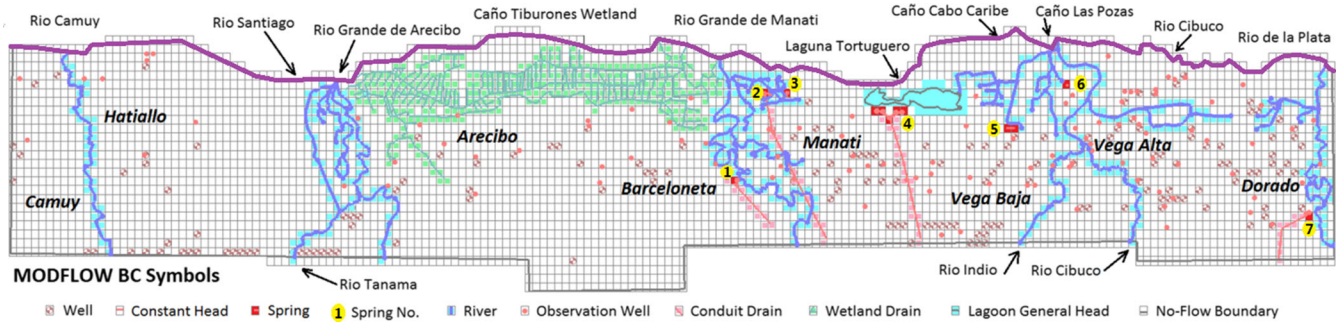

Fig. 5 Setup of numerical groundwater model, location of municipalities, model grid and boundaries, rivers, pumping wells, monitoring wells, springs, drainage lines, the lake and the wetland

region. Location of springs, sinkholes, dip directions, dry valleys, strikes, and partially mapped surface lineaments were initially considered as features along which drainage may have a major controlling influence on regional groundwater flow. Among different scenarios, however, only drain lines connecting sinkholes to springs are assumed to be significant and are included in the model (red lines in Fig. 5). Such drain lines were not necessarily along other superficial features and were selected by following the shortest path between springs and sinkhole areas. Primarily developed to simulate agricultural drainage systems, the drain feature in MODFLOW removes water from an aquifer at a rate proportional to the head difference between the water table and the drain elevation. The drain feature is effective as long as the water level in aquifer is above the drain elevation (Harbaugh et al. 2000).

The major streams flowing through the study area are Rio Camuy, Rio Santiago, Rio Tanama, Rio Grande de Arecibo, Rio Grande de Manati, Rio Indio, Rio Cibuco, and Rio de la Plata (the longest in the island). The streams are implemented as a transfer (Cauchy) boundary condition with constant water level stages and riverbed conductance values. Withdrawal rates, riverbed conductance and river stages were taken from previous studies (Gomez-Gomez and Torres-Sierra 1988; Torres-González et al. 1996; Sepúlveda 1996; Rodríguez-Martínez 1996; Cherry 2001).

Model calibration

Model calibration is performed using the parameter estimation routine PEST (Doherty et al. 1994) linked with MODFLOW and integrated in GMS. In the steady-state calibration process, the optimization procedure is based on automatic minimizing of the deviations between calculated and measured heads. A zonation of the calibration parameters (i.e., recharge and hydraulic conductivity) was applied based on similar geologic characteristics (e.g. lithology, topography, and surface drainage) and the study scale (i.e. regional). During the PEST calibration process, the parameter values were adjusted within predefined ranges until the simulated heads matched the observed heads as well as possible by minimizing the sum of squared deviations between simulated and observed heads at the observation wells. Due to data limitation, uniform values for the effective porosity (0.3), specific yield (0.05), and storage coefficient (10^{-5} m^{-1}) are defined in a transient calibration using continuously measured water level data of USGS observation wells.

After the recharge and hydraulic conductivity values are optimized using the EPM approach, connected pathways of drain cells are added to the modeling domain to simulate the drainage effects of conduits and improve the modeling efficiency. Different conceptually realistic scenarios for location of drain lines are considered, connecting the few springs near the north coast and classified as conduit-type by Rodriguez-Martinez (1997) (surficial discharge points) to the known zones of surficial karst features (sinkholes, dolines, etc.) in the south. In each scenario, the upgradient ends of the drain lines were aligned along surface lineaments (Ward et al. 1991), major dry valleys (Monroe 1976), or rows of sinkholes, which frequently occur in the south in Aguada limestone (Monroe 1980). Water levels in the 101 monitoring wells provided sufficient hydraulic head data from the year 1992 in high spatial resolution (Torres-González et al. 1996; Sepúlveda 1999; Cherry 2001) for manually evaluating the impact of simulated drains on simulation results. The drain lines directly connecting sinkholes to springs were found to significantly improve the simulated water table, and the drain specific parameters were further adjusted during the manual calibration.

A sensitivity analysis is performed to evaluate the dependency of drainage rate and modeling error to two lumped parameters, the drainage conductance and the head difference with the surrounding water table. Since the drainage rate is a function of both parameters, one can be kept constant and the other can be calibrated. A high drainage conductance (a lumped parameter representing the average conductance of the material surrounding the drain) was assigned for all drain lines, and the drainage elevations were manually adjusted until the overall simulation error was minimized. While lower values of drain conductance can limit the drainage capacity (Fig. 6a), a high conductance of 100 m^2/d/m was used to enhance the removal of water from the simulated conduits by ensuring full drainage capacities and to eliminate the need for unknown conduit specific data. Similar to Quinn et al. (1998), the drain elevation at the discharge point of each drain line was assumed to be equal to the elevation of the associated spring, and also assumed to be below the steady-state water table upstream of the spring. Upstream elevations were estimated from borehole logs, potentiometric surface and geologic formation maps, and then were adjusted during calibration. The upstream drain elevations were manually calibrated for all drain lines simulated in the model, ensuring active flow in all inferred drains, reaching expected steady-state discharge and minimizing the total root mean squared error (RMSE; Fig. 6b). Similar to Yobbi (1989), a head-dependent drain feature is used to simulate springs classified as diffuse-type by Rodriguez-Martinez (1997), where steady-state discharge is a linear function of the head difference between the spring and the potentiometric surface in the aquifer.

Results

Regional hydrogeology

While a uniformly distributed hydraulic conductivity fails to represent the steady-state water table in this spatially

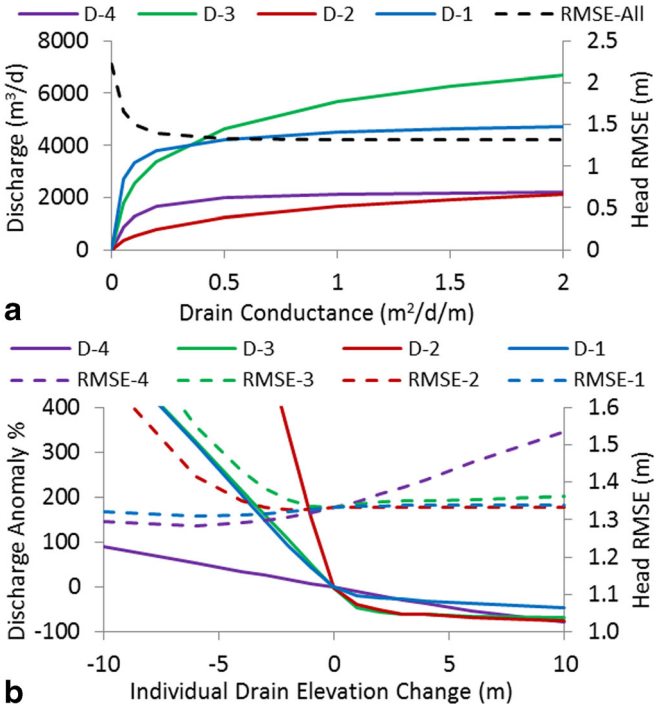

Fig. 6 Sensitivity of steady-state spring discharge and steady-state calibration RMSE to changes in: **a** uniform drain conductivity; and **b** individual drain elevations. *D-1* to *D-4* corresponds to the drains connected to spring Nos. 1–4 (Table 1), respectively

heterogeneous karst aquifer (RMSE of 10.01 m), automatically calibrated hydraulic conductivities of discrete zones significantly increase the simulation's accuracy (RMSE of 2.08 m). The chosen zoning corresponds to the distribution of geological formations (Torres-González et al. 1996; Sepúlveda 1999; Cherry 2001). Maximum transmissivities of the upper aquifer are calibrated as 3,800, 10,400, 5,100, 6,500, 8,600, and 8,900 m^2/d in the karst uplands of eastern Hatillo, Arecibo, eastern Manati, Vega Baja, eastern Vega Alta and western Dorado, respectively. The transmissivity values are largely controlled by the aquifer thickness and are reduced to less than 450 m^2/d near alluvial deposits and less than 50 m^2/d along the southern boundaries of the study area where the aquifer lenses out above the Cibao formation. It also significantly decreases toward the north boundary where the aquifer thickness is reduced by the saltwater interface at the coast.

The calibration is further improved by adding four drain lines connecting southern sinkholes with springs classified as conduit-type by Rodriguez-Martinez (1997), decreasing the RMSE from 2.08 to 1.33 m (Fig. 7). This approach lowered the local water table and resulted in a better match between the simulated and observed hydraulic head. Individually lowering elevations of four drain lines (D-1, D-2, D-3, D-4) by 1 m results in a raise of 7,190, 4,370, 8,800 and 1,980 m^3/d in the respective spring's discharge, while slightly altering the overall modeling RMSE, which leads to different anomalies in the expected spring discharges, e.g. it almost quadruples the discharge for spring No. 2 (see Table 1). Figure 8 shows that the simulated hydraulic heads at upstream of spring No. 3 in the steady-state conditions for the EPM model after and before switching from the spring-representing drain cells to the conduit-representing drain line.

Spring hydrographs

Measured and simulated hydrographs of two springs, i.e. Oje de Agua and Oje de Guillo, are plotted as a response to daily rainfall at Manati rain gauge station for a duration of 33 months (Fig. 9). Both spring hydrographs show similar responses to rainfall events, i.e. a steep limb rising to the peak, and a recession limb that is less steep than the rising limb. A time lag of about 3–12 days between the rainfall event and the peak of the hydrograph can be observed, as expected in highly permeable aquifers. The steep slopes of the recession curves immediately after the peak indicate fast drainage (quick flow) from conduits, while the subsequent gentle slopes toward the end of recession curves represent diffuse drainage (slow flow) through smaller fractures and the rock matrix. Simulated hydrographs roughly represent the shape and intensity of the measured hydrographs, but fail to reproduce very high spring discharges up to 5×10^4 m^3/d.

Classified as a diffuse-type spring by Rodriguez-Martinez (1997), with a catchment area of about 10 km^2 and an estimated annual subregional recharge rate of about 510 mm/year, Oje de Agua spring (18°26′57″N 66°25′06″W) provides a base flow of about 5,000–10,000 m^3/d. This perennial spring flows even during periods of low rainfall and exhibits some seasonal variations with moderate to strong responses to small rainfall events (e.g. 7/93 and 2/94); therefore, as also discussed by White (2002), this low-variability spring may

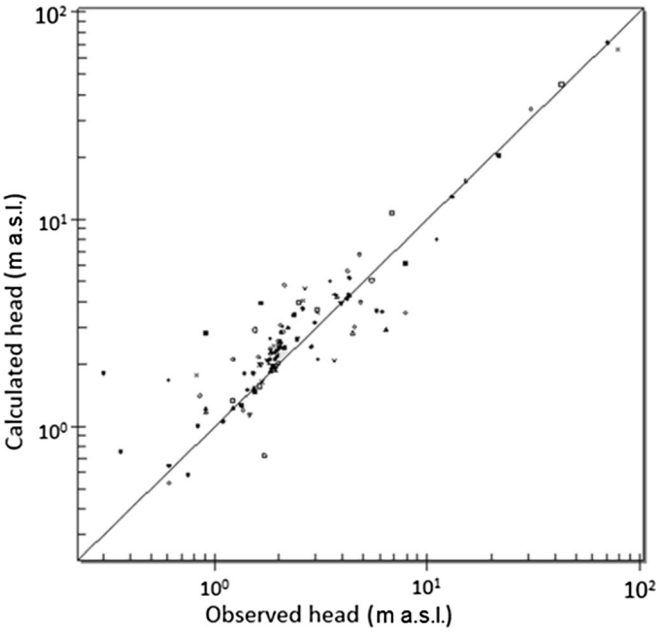

Fig. 7 Scatter calibration diagram of simulated versus observed hydraulic head for steady-state calibration of the flow model with drain lines

be connected to a conduit network. During the long dry period of 1994–1995, there is a decline in base flow, and seasonal variations of the spring discharge are less intense. Extreme rainfalls are often in the wet season (October to January), causing high historical spring discharges of up to 50,000 m^3/d.

Classified as conduit-type spring by Rodriguez-Martinez (1997), Oje de Guillo spring exhibits stronger (more sudden and sharp) responses to extreme short-term rainfall events (e.g. 11/93 and 8/95) than Oje de Agua spring. Its catchment area varies depending on hydrogeological conditions. Its base flow, which ranges between 1,500 to 3,000 m^3/d, is much lower compared to Oje de Agua spring. The recession limb of this spring is much steeper compared to Oje de Agua spring, indicating relatively short residence time in the conduit network. While the terms conduit-type and diffuse-type springs are widely used in the literature, they only indicate the extreme opposite ends of the flow range (e.g. White 2002). Both springs in this study are believed to be fed by conduits, and the differences in their responses are likely largely the result of recharge differences, with a higher proportion of concentrated recharge at sinkholes and dolines for the Ojo de Guillo spring. Other studies such as Quinn et al. (1998) only compared the average

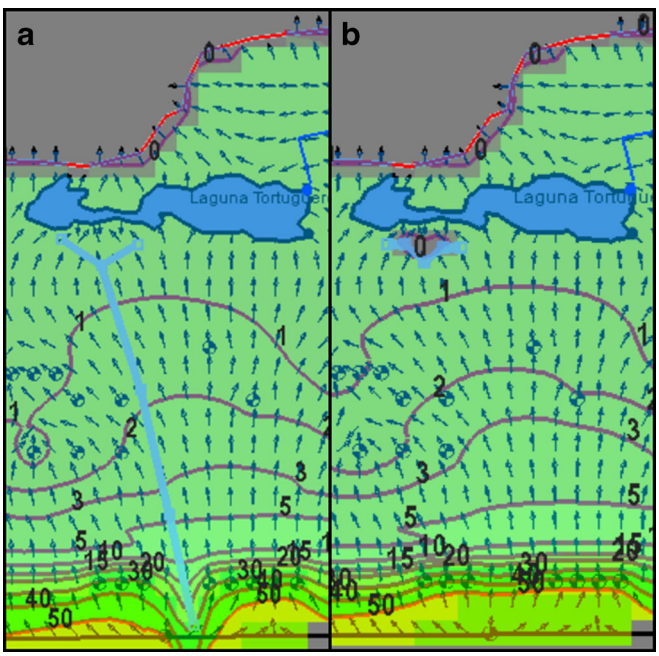

Fig. 8 Simulated hydraulic heads around Laguna South spring (see Table 1) using EPM model with drain cells (**b**) compared with the EPM model with drain lines (**a**) to represent the conduit. The *contours* represent lines of equal hydraulic head (m a.s.l.) around a drain pathway

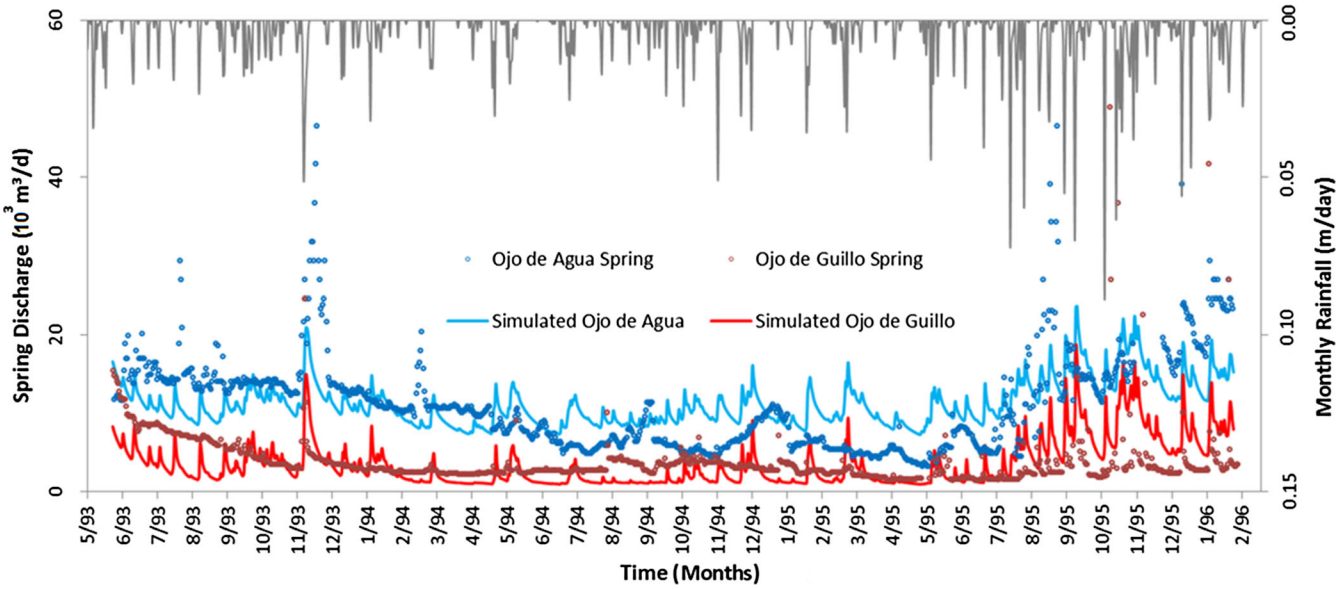

Fig. 9 Daily rainfall hyetograph vs. simulated and observed daily mean discharge hydrograph between June 1993 and February 1996 for *Oje de Agua* spring in Vega Baja and *Oje de Guillo* spring in Manati

simulated spring discharges from the calibrated model with one-time spring gauging measurements.

Hydraulic head

The western part of the model has slightly higher groundwater levels due to receiving more rainfall, fewer pumping wells and fewer natural drainage features (e.g. conduits, springs, lagoons, wetlands, etc.). The hydraulic gradient in the middle zone of Aymamon limestone is flat (0.5–1.5 m/km) because of the relatively high hydraulic conductivity in this area. From north to south, the Aguada limestone, Cibao formation, Lares limestone and San Sebastian formation underlie the Aymamon limestone, reflecting the changing hydraulic conductivities. Lower conductivity in the lower part of the Aymamon and within the Aguada limestone, gradually increases the hydraulic gradient up to about 47 m/km (about 6.5 km inland from the coast). Even farther to the south, the underlying impermeable Cibao formation gradually adjusts the gradient to follow the slope of the topography (about 8 km inland from the coast).

Longitudinal hydraulic head profiles for six springs are drawn using the calibrated model (Fig. 10) to provide a cross-sectional view of the upgradient head distribution. The impermeable Cibao formation rises toward the south of the aquifer, thus water levels significantly rise as well. From the south, as transmissivity increases halfway through the north, the water level decreases, and the downgradient flow is lessened. This is because groundwater discharges to pumping wells, conduits, diffuse springs, the Tortuguero lagoon, and the Caño Tiburones wetland. Pumping wells subtract a significant portion of subsurface flow by capturing the water which would otherwise discharge to natural water bodies. Closer to the coast, the hydraulic gradient slightly increases and the transmissivity declines; however the overall northward groundwater flow decreases because the hydraulic gradient is not sufficient to overcome the effects of lessened transmissivity.

Groundwater budgets

Groundwater recharge in the model is mostly from infiltration of rainfall, followed by river leakage through streambeds and from unconfined parts of the lower aquifer in the south. The rivers collect and carry rain and runoff from the land and flow predominantly north to the Atlantic Ocean. Model outflows are composed of spring discharges, discharge to the ocean at the northern model boundary and discharge into wetland areas, where the water is drained by channel networks and pumped into the ocean. Major sinks in the water budget are groundwater withdrawals by wells. The calibrated model's water budget indicates that roughly 11 % of the water that enters the karst system as recharge exits as conduit or diffuse flow at the springs. The resulting conduit discharge is lower than that in most of other karst systems elsewhere such as the Malm Formation with conduit discharge of 25–70 % of total groundwater flux (Weise et al. 2001). The simulated aquifer interactions with surface water and the steady-state groundwater budget for the year 1992 is summarized in Table 2.

Discussion

In the scenic karst topography of NPR, coastal groundwater is consumed continuously as the main source for domestic,

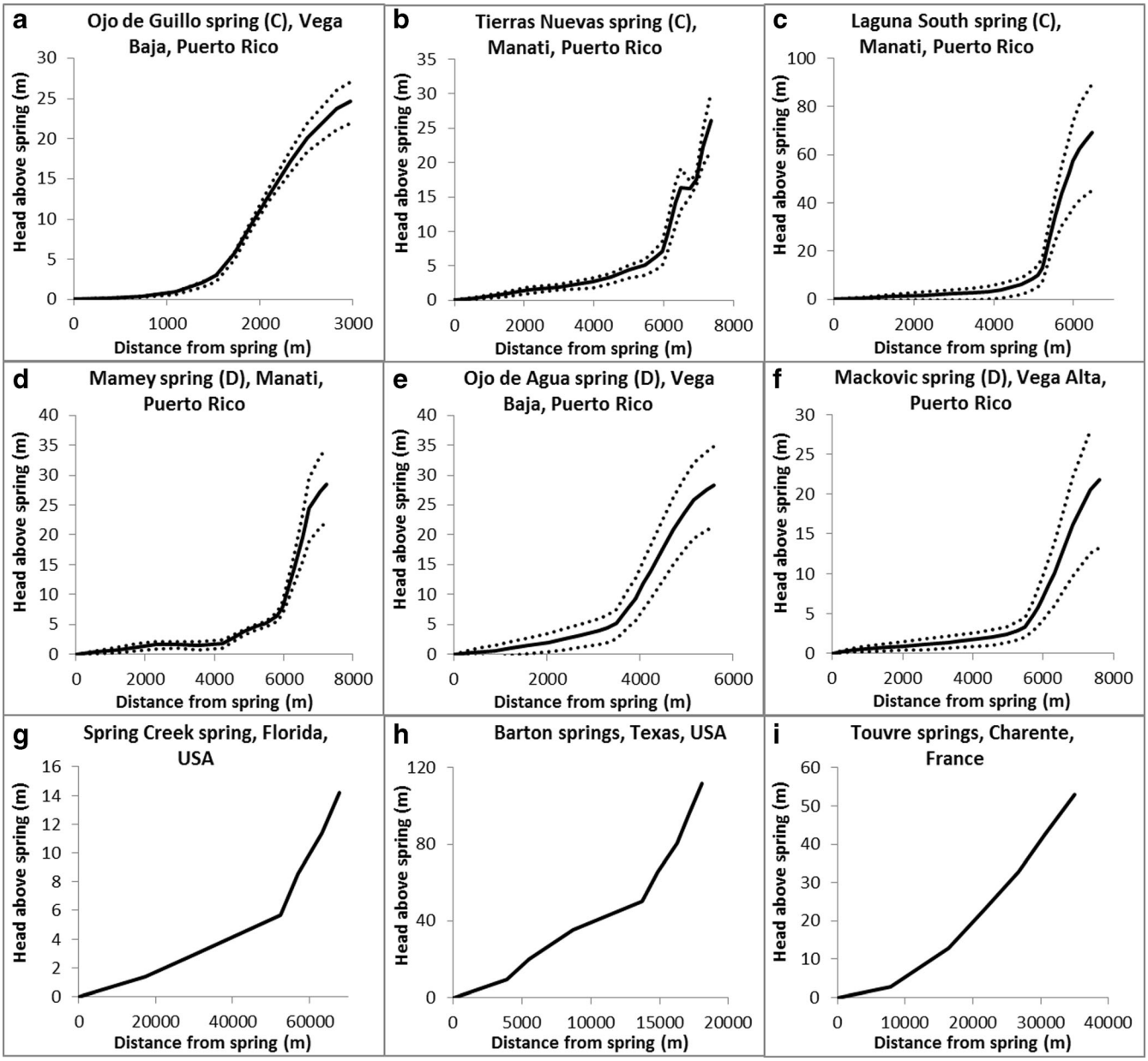

Fig. 10 Longitudinal head profiles upgradient of six major springs of the study (**a**–**f**) for the calibrated model (*solid lines*) and for 50 % increase and decrease in recharge (*dotted lines*); compared with three productive springs in other karst systems (**g** Davis 1996; **h** Slade et al. 1985; **i** Larocque et al. 1999)

industrial, and agricultural water use. The simulated potentiometric surface agrees with overall northward regional flow directions, but they demonstrate slight depressions in the middle and localized depressions in southern parts resulting from the influence of the draining conduits. The influence of conduits on the simulated potentiometric surface is clearly demonstrated in Fig. 8. Conduits act as a hydraulic sink by draining the matrix especially in the southern area and the simulated hydraulic gradient is directed from matrix to conduits. In the northern part, local changes in the direction of groundwater flow illustrate the interaction of groundwater with the lake and the tendency of surface-water bodies to dominate the groundwater levels. This study suggests that the influence of conduits is a key factor influencing groundwater flow in the karst aquifers of central NPR.

Drain characteristics in this study do not represent the actual properties of the conduits, e.g. accurate locations, roughness, diameter, tortuosity, and lumped matrix-conduit exchange coefficients; however, the drains simulate the drainage effect of the conduits on the regional flow field, thus improving the accuracy of the EPM approach. Just like conduits, the drains act as low hydraulic-resistance features, forcing the flow field in the surrounding matrix and fracture system toward the drainage.

Table 2 Steady-state groundwater budgets for 1992 hydrologic conditions in the central NPR

	m^3/d	%
Inflows		
Recharge	270,650	76.8
River leakage	62,090	17.6
Subsurface contributions	19,600	5.6
Total inflow	352,340	100
Outflows		
Withdrawals	149,500	42.4
Springs	30,120	8.6
Ocean discharge	72,030	20.4
Wetland drainage	93,700	26.6
Lake	6,990	2.0
Total outflows	352,340	100

Springs are characteristic features of karst terrains and estimating the hydrographs (discharge rates) and chemographs (water compositions) is essential in managing karst groundwater resources. This investigation suggests that in NPR, variations in spring discharge reflect the response of the aquifer to recharge events. The magnitude of such variations also depends on the size of the groundwater reservoir, i.e., smaller reservoirs show higher variations (Singhal and Gupta 2010). Even if karst springs are fed by conduits, they may exhibit little or no hydrograph response to storms due to primary storage in the epikarst, as also noted by White (2007). Spring discharges in karst aquifers can demonstrate highly variable flow depending on recent climate conditions.

Although the seven major springs in the central NPR were classified either as diffuse type or conduit type, this study's simulation suggests that the studied karst springs are combinations of both types. Studies suggest that in addition to conduit flow, matrix flow contributes significantly to spring flow (e.g. Florea and Vacher 2006). When little to no data on internal geometry and flow conditions is available, the lumped approach is an efficient alternative to simulate spring hydrographs from rainfall at short time scales because it estimates the output based on the input without requiring investigation of the exact nature of the karst system. If the exact subsurface geometry and physical properties of conduits are known, physical models may provide reasonable results for spring response and behavior; however, high internal heterogeneity and lack of knowledge about spring systems limit the ability of classical EPM models like MODFLOW to accurately simulate the actual karst behavior.

The proper application of the methodology used in this study depends on the study scale. While scale effects could be seen in porous aquifers, hydraulic conductivity values in karst aquifers calculated from slug tests show more dependency on the measurement scale, which imposes additional uncertainty in karst hydrogeology (e.g. Rovey and Cherkauer 1995). Hydraulic conductivities within NPR karst system are found to be scale dependent and significantly increase with higher test radius. Applicability of the EPM approach in regional-scale groundwater modeling within karst environments depends upon sufficiently enhancing the equivalent conductivities based on the modeling scale; therefore, caution must be taken when using values established by laboratory tests or for modeling purposes at the field scale.

Simplification of complex recharge and flow mechanisms in this karst aquifer using an EPM modeling approach for the fractured matrix along with drainage lines representing conduits limit the accuracy of simulated discharge. The drainage feature is also limited in addressing the two-way fluid exchange between matrix and conduit network. A real conduit system is much more complex than the simplified drains used in this model and its behavior is in addition influenced by rapid turbulent flow after extreme rainfall events, which is not considered in the approach. The selected pathways are simplifications of the true channel network. A more accurate connectivity study of sinkholes in the south of the study area to active springs in the north would require more field investigations such as tracer tests in the area. Other inaccuracies may arise from the temporal recharge data based on rainfall in Manati station being 10 km outside the spring catchment area, and from assuming constant pumping rates for withdrawal wells.

To examine whether the attributes of NPR karst system are common in carbonate aquifers, a comparison was made with examples of highly productive springs from the literature. The three chosen groundwater basins are from Florida and Texas in the US and Charente in France. Head profiles along major troughs were estimated from detailed potentiometric-surface maps upstream of major springs (Fig. 10g–i). Touvre springs (Larocque et al. 1999), with the second largest spring flow (1.12×10^6 m^3/d) after the Fountain of Vaucluse, are fed by La Rochefoucauld karst in France. As one of the two largest karst springs in Florida, Spring Creek (4.89×10^6 m^3/d; Davis 1996) consists of several first-order coastal springs fed by Floridan aquifer. Barton Springs (0.13×10^6 m^3/d; Slade et al. 1985), the fourth largest spring in central Texas, consists of four springs fed from the Edwards Aquifer. Similar to this study, groundwater modeling efforts for those springs show that aquifer transmissivity increases down gradient towards the springs; however in the NPR karst system, the longitudinal head profiles are sharper along the interface of saltwater with Cibao formation where the groundwater lens is thickest (about 2 km north of southern model boundary). The profiles' incurvature indicates the presence of similar characteristics between karst aquifers in the central NPR with those elsewhere, and therefore hydrogeologic conditions presented herein could parallel other karst systems in the world.

The head profiles resulting from half an order of magnitude increase and decrease in recharge demonstrate the sensitivity of water levels to climate conditions. A higher recharge rate not only significantly increases the discharge to natural drainage features, but also raises the water table. The effects of such climatic stresses become more obvious farther from the springs. The magnitude of seasonal fluctuations depends upon the distance from the ocean as a constant head boundary. Further examination of the model resulting from alteration in calibrated hydraulic conductivity suggested significant influence of geology on the head profiles. The head profile for Tierras Nuevas spring in Manati (Fig. 10b) captures a local peak about 17 m a.s.l., which represents a depression caused by a passing conduit. At a local scale, there is not enough data to validate the flow dominance by conduits as an example of the impact of scale on the applicability of the EPM approach.

Conclusions

While the field data sparsity often limits the ability to locate and characterize the conduit system, this paper introduces a method for modeling the heterogeneities of flow in karst aquifers by assigning arrays of adjacent model cells with drains to simulate conduits. In NPR, the aquifer permeability is certainly affected but does not become largely dominated by distinguishable channel networks that control the groundwater flow. This is partially due to the high rate of groundwater withdrawals which, compared to natural conditions, lower the potentiometric surface and control the local subsurface hydrodynamics. The drainage feature simulates the drainage effect of conduits by influencing the nearby water-table levels, but it is incapable of capturing the rapid conduit flow or the fluid exchange between the matrix and the conduit network. With improved and more refined field data (from tracer tests, remotely sensed images, geophysical surveys, spring and well investigations) the current approach could advance to an even more powerful technique for evaluating karst groundwater resources and conceptual hydrogeological models

Acknowledgements We thank Dr. Rachel Grashow and Ms. Christine Gordon for their editorial help on the paper. We also thank the editor and the anonymous reviewers for their valuable comments. Support of the work described is provide through award No. P42ES017198 from the National Institute of Environmental Health Sciences to the PROTECT research project. The content is solely the responsibility of the authors and does not necessarily represent the official views or policies of the National Institute of Environmental Health Sciences or the National Institute of Health.

References

Alemán-Gonzalez WB (2010) Karst map of Puerto Rico. US Geol Surv Open File Rep 2010-1104

Angelini P, Dragoni W (1997) The problem of modeling limestone springs: the case of Bagnara (North Apennines, Italy). Ground Water 35(4):612–618

Aquaveo (2014) Groundwater modeling system (GMS, v.10), Aquaveo, Provo, UT

Bennett GD, Giusti EV (1972) Ground water in the Tortuguero area, Puerto Rico: as related to proposed harbor construction. US Geol Surv Water Resour Bull 10:25

Briere PR, Scanlon KM (2000) Lineaments and lithology derived from a side-looking airborne radar image or Puerto Rico. In: Puerto Rico: marine sediment database, terrestrial and sea-floor imagery and tectonic interpretations. US Geol Surv Open File Rep 00-006

Butscher C, Auckenthaler A, Scheidler S, Huggenberger P (2011) Validation of a numerical indicator of microbial contamination for Karst springs. Ground Water 49(1):66–76

Calvesbert RJ (1970) Climate of Puerto Rico and U.S. Virgin Islands. Climate of the states. Climatography of the United States no. 60–52. U.S. Dept of Commerce, Environmental Science Services Admin., Washington, DC

Cherry GS (2001) Simulation of flow in the upper north coast limestone aquifer, Manatí-Vega Baja area, Puerto Rico. US Geol Surv Water Resour Invest Rep 00-4266

Davis H (1996) Hydrogeologic investigation and simulation of groundwater flow in the Upper Floridan aquifer of north-central Florida and southwestern Georgia and delineation of contributing areas for selected City of Tallahassee, Florida, water-supply wells. US Geol Surv Open-File Rep 95-4296

Deike RG (1969) Relations of jointing to orientation of solution cavities in limestones of central Pennsylvania. Am J Sci 267(10):1230–1248

Doherty J, Brebber L, Whyte P (1994) PEST: model-independent parameter estimation. Watermark Computing, Brisbane, Australia

Dufresne DP, Drake CW (1999) Regional groundwater flow model construction and wellfield site selection in a karst area, Lake City, Florida. Eng Geol 52:129–139

Eisenlohr L, Bouzelboudjen M, Kiraly L, Rossier Y (1997) Numerical versus statistical modeling of natural response of a karst hydrogeological system. J Hydrol 202(1):244–262

Florea LJ, Vacher HL (2006) Springflow hydrographs: eogenetic vs. telogenetic karst. Ground Water 44(3):352–361

Garven G (1995) Continental-scale groundwater flow and geologic processes. Annu Rev Earth Planet Sci 23:89–118

Ghasemizadeh R, Hellweger F, Butscher C, Padilla I, Vesper D, Field M, Alshawabkeh A (2012) Review: Groundwater flow and transport modeling of karst aquifers, with particular reference to the North Coast Limestone aquifer system of Puerto Rico. Hydrogeol J 20(8):1441–1461

Ghasemizadeh R, Yu X, Butscher C, Hellweger F, Padilla I, Alshawabkeh A (2015) Equivalent porous media (EPM) simulation of groundwater hydraulics and contaminant transport in karst aquifers. PloS One 10(9):e0138954

Giusti EV (1978) Hydrogeology of the karst of Puerto Rico: USGS Professional Paper 1012, p 68

Giusti EV, Bennett GD (1976) Water resources of the north coast limestone area. US Geological Survey Water-Resources Investigations 42–75, Puerto Rico, p 42

Gomez-Gomez F, Torres-Sierra H (1988) Hydrology and effects of development on the water-table aquifer in the Vega Alta quadrangle. US Geol Surv Water Resour Invest Rep 87-4105, 53 pp

Graf T, Therrien R (2007) Variable-density groundwater flow and solute transport in irregular 2D fracture networks. Adv Water Resour 31;30(3):455–468

Guzmán-Ríos S (1988) Hydrology and water quality of the principal springs in Puerto Rico. US Geol Surv Water Resour Invest Rep 85-4269, 30 pp

Harbaugh AW, Banta ER, Hill MC, McDonald MG (2000) MODFLOW-2000, the U.S. geological survey modular ground-water model: user guide to modularization concepts and the ground-water flow process. US Geol Surv Open File Rep 00-92

Hurd TM, Brookhart-Rebert A, Feeney TP, Otz MH, Otz IN (2010) Fast, regional conduit flow to an exceptional-value spring-fed creek: implications for source-water protection in mantled karst of south-central Pennsylvania. J Cave Karst Stud 72(3):129–136

Jukić D, Denić-Jukić V (2009) Groundwater balance estimation in karst by using a conceptual rainfall-runoff model. J Hydrol 373(3–4): 302–315

Kaufmann G, Braun J (1999) Karst aquifer evolution in fractured rocks. Water Resour Res 35(11):3223–3238

Kiraly L (1975) Rapport sur l'état actuel des connaissances dans le domaine des caractères physiques des roches karstiques. Hydrogeology of Karstic Terrains 3:53–67

Kovacs A (2003) Geometry and hydraulic parameters of karst aquifers: a hydrodynamic modeling approach. PhD Thesis, CHYN, Univ de Neuchâtel, Switzerland

Larocque M, Banton O, Ackerer O, Razack M (1999) Determining karst transmissivities with inverse modeling and an equivalent porous media. Ground Water 37:897–903

Lattman LH, Parizek RR (1964) Relationship between fracture traces and the occurrence of groundwater in carbonate rocks. J Hydrol 2(2):73–91

Lauritzen SE, Odling N, Petersen J (1992) Modeling the evolution of channel networks in carbonate rocks. ISRM Symp Eurock 92:57–62

Lee ES, Krothe NC (2001) A four-component mixing model for water in a karst terrain in south-central Indiana, USA using solute concentration and stable isotopes as tracers. Chem Geol 179:129–143

Liedl R, Sauter M, Hückinghaus D, Clemens T, Teutsch G (2003) Simulation of the development of karst aquifers using a coupled continuum pipe flow model. Water Resour Res 39(3):1057

Lugo AE, Castro LM, Vale A et al (2001) Puerto Rican karst: a vital resource. General technical report, WO-65, USDA Forest Service, Washington, DC

Mcdonald MG, Harbaugh AW (1988) A modular three-dimensional finite-difference groundwater flow model. US Geological Survey Techniques of Water-Resources Investigations, book 6, chapter A1, 586 pp, USGS, Reston, VA

Meinzer OE (1927) Large springs in the United States. US Geol Surv Water Supl Pap 557, 94 pp

Monroe WH (1976) The karst landforms of Puerto Rico. US Geol Surv Prof Pap 899, 69 pp

Monroe WH (1980) Geology of the middle Tertiary formations of Puerto Rico. US Geol Surv Prof Pap 953

Neuman SP (1990) Universal scaling of hydraulic conductivities and dispersivities in geologic media. Water Resour Res 26(8):1749–1758

O'Leary DW, Freidman JD, Pohn HA (1976) Lineament, linear, lineation: some proposed new definitions for old terms. Geol Soc Am Bull 87:1463–1469

Papadopoulou MP, Varouchakis EA, Karatzas GP (2010) Terrain discontinuities effects in the regional flow of a complex karstified aquifer. Environ Model Assess 15(5):319–328

Peterson EW, Wicks CM (2006) Assessing the importance of conduit geometry and physical parameters in karst systems using the storm water management model (SWMM). J Hydrol 329(1):294–305

Puig JC, Rodríguez JM, Rodríguez-Martínez J (1993) Ground-water resources of the Caguas-Juncos valley, Puerto Rico. US Geol Surv Water Resour Invest Rep 91-4079

Quinn J, Tomasko D, Glennon MA, Miller SF, McGinnis LD (1998) Using MODFLOW drains to simulate groundwater flow in a karst environment. Argonne National Lab, Lemont, IL

Quinn JJ, Tomasko D, Kuiper JA (2006) Modeling complex flow in a karst aquifer. Sedimen Geol 184(3–4):343–351

Quinones-Aponte V (1986) Water resources of the lower Rio Grande de Arecibo alluvial valley, Puerto Rico. US Geol Surv Water Resour Invest Rep 85-4160

Renken RA, Ward WC, Gill IP, Gómez GF, Rodríguez JM et al (2002) Geology and hydrogeology of the Caribbean Islands aquifer system of the commonwealth of Puerto Rico and the US Virgin Islands. US Geol Surv Prof Pap 1419, 139 pp

Rodríguez-Martínez J (1995) Hydrogeology of the North Coast limestone aquifer system of Puerto Rico. US Geological Survey Water Resources Report 94-4249, p 22

Rodríguez-Martínez J (1996) Hydrogeology and ground-water/surface-water relations in the Bajura area of the Municipio of Cabo Rojo, southwestern Puerto Rico. US Geol Surv Water Resour Invest Rep 95-4159

Rodriguez-Martinez J (1997) Characterization of springflow in the North Coast Limestone of Puerto Rico using physical, chemical, and stable isotopic methods. US Geol Surv Water Resour Invest Rep 97-4122

Rovey CW II (1994) Assessing flow systems in carbonate aquifers using scale effects in hydraulic conductivity. Environ Geol 24(4):244–253

Rovey CW, Cherkauer DS (1995) Scale dependency of hydraulic conductivity measurements. Groundwater 33(5):769–780

Sauter M, Kovacs A, Geyer T, Teutsch G (2006) Modellierung der Hydraulik von karst Grundwasserleiter: eine Übersicht [Modeling of the hydraulics of karst aquifers: an overview]. Grundwasser 11(3):143–156

Scanlon BR, Mace RE, Barret ME, Smith B (2003) Can we simulate regional groundwater flow in a karst system using equivalent porous media models? Case study, Barton springs Edwards Aquifer, USA. J Hydrol 276(1–4):137–158

Schindel GM, Quinlan JF, Davies G, Ray JA (1996) Guidelines for wellhead and springhead protection area delineation in carbonate rocks. USEPA 904-B-97-003, US EPA, Washington, DC, 126 pp

Sepúlveda N (1996) Three-dimensional ground-water-flow model of the water-table aquifer in Vega Alta, Puerto Rico. U.S. Geological Survey. Water-Resources Investigations Report 95–4184

Sepúlveda N (1999) Ground-water flow, solute transport, and simulation of remedial alternatives for the water-table aquifer in Vega Alta, Puerto Rico. US Geol Surv Water Resour Invest Rep 97-4170

Shuster ET, White WB (1971) Seasonal fluctuations in the chemistry of limestone springs: a possible means for characterizing carbonate aquifers. J Hydrol 14(2):93–128

Singhal BBS, Gupta RP (2010) Hydrogeology of carbonate rocks. Appl Hydrogeol Fractur Rock. Springer Netherlands, Houten, Netherlands, pp 269–289

Slade RM Jr, Ruiz LM, Slagle DL (1985) Simulation of the flow system of Barton Springs and associated Edwards aquifer in the Austin area, Texas. US Geol Surv Water Resour Invest Rep 85-4299, 49 pp

Smart PL, Hobbs SL (1986) Characterization of carbonate aquifers: a conceptual base. Proceedings of the Environmental Problems in Karst Terranes and their Solutions conference, Bowling Green, KY, October 1986, pp 1–14

Snow D (1965) A parallel plate model of fractured permeable media. PhD Thesis, University of California, Berkeley, CA

Teutsch G, Sauter M (1991) Groundwater modeling in karst terranes: scale effects, data acquisition and field validation. Proceeding of Third Conf. Hydrogeology, Ecology, Monitoring, and Management of Ground Water in Karst Terranes, Nashville, TN, December 1991, pp 17–35

Torres-González A (1985) Simulation of ground-water flow in the water table aquifer near Barceloneta, Puerto Rico. US Geol Surv Water Resour Invest Rep 84-4113

Torres-González S, Planert M, Rodríguez MJ (1996) Hydrogeology and simulation of ground-water flow in the upper aquifer of the Río

Camuy to Río Grande de Manatí area, Puerto Rico. US Geol Surv Water Resour Invest Rep 95-4286

Tucci P, Martínez MI (1995) Hydrology and simulation of ground-water flow in the Aguadilla to Rio Camuy area, Puerto Rico. US Geol Surv Water Resour Invest Rep 95-4028

Wanakule N, Anaya R (1993) A lumped parameter model for the Edwards aquifer. Technical report 163, Texas Water Resources Institute, College Station, TX, 84 pp

Ward WC, Scharlach RA, Hartley JR (1991) Controls on porosity and permeability in subsurface Tertiary carbonate rocks of northern Puerto Rico. In: Gómez Gómez, Fernando, Quinones Aponte, Vicente, and Johnson, AI (eds) Regional aquifer systems of the United States: aquifers of the Caribbean Islands. American Water Resources Association Monograph Series 15, American Water Resources Association, Middelburg, VA, pp 17–23

Weatherhill D, Graf T, Simmons CT, Cook PG, Therrien R, Reynolds DA (2008) Discretizing the fracture-matrix interface to simulate solute transport. Ground Water 46(4):606–615

Weise SM, Rau I, Seiler KP (2001) Long-term storage behaviour of karstic aquifer deduced by multi-trace investigations. EGS XXVI General Assembly, European Geophysical Society, Nice, France

White WB (1969) Conceptual models for carbonate aquifers. Groundwater 7(3):15–21

White WB (2002) Karst hydrology: recent developments and open questions. Eng Geol 65(2):85–105

White WB (2003) Conceptual models for karstic aquifers. Speleolog Evolut Karst Aquifers 1(1). http://www.speleogenesis.info/directory/karstbase/pdf/seka_pdf4491.pdf. Accessed 30 January 2015

White WB (2007) Cave sediments and paleoclimate. J Cave Karst Stud 69(1):76–93

White WB, White EL (2001) Conduit fragmentation, cave patterns and the localization of karst ground water basins: the Appalachians as a test case. Theor Appl Karst 13–14:9–23

Worthington SRH (1991) Karst hydrogeology of the Canadian Rocky Mountains. PhD Thesis, McMaster University, Hamilton, ON, 227 pp

Worthington SRH (2009) Diagnostic hydrogeologic characteristics of a karst aquifer (Kentucky, USA). Hydrogeol J 17(7):1665–1678

Worthington SRH, Ford DC (2009) Self-organized permeability in carbonate aquifers. Ground Water 47(3):326–336

Yobbi D (1989) Simulation of steady-state ground water and spring flow in the upper Floridian aquifer of coastal Citrus and Hernando counties, Florida. US Geol Surv Water Resour Invest Rep 88-4036

Yu X, Ghasemizadeh R, Padilla IY, Irizarry C, Kaeli D, Alshawabkeh AN (2015a) Spatiotemporal changes of CVOC concentrations in karst aquifers: analysis of three decades of data from Puerto Rico. Sci Total Environ 511:1–10

Yu X, Ghasemizadeh R, Padilla IY, Meeker JD, Cordero JF, Alshawabkeh AN (2015b) Sociodemographic patterns of household water-use costs in Puerto Rico. Sci Total Environ 524:300–309